

# Multiple Isomerization of Structural Units in Ion-Polymeric Heteronuclear Gold(III)–Zinc(II) Complex ( $[\text{Au}\{\text{S}_2\text{CN}(\text{C}_4\text{H}_9)_2\}_2]_2[\text{ZnCl}_4]_n$ ): Chemisorption-Based Synthesis, Supramolecular Structure (Self-Organization of Long-Period Cation–Cationic Polymer Chains), and Thermal Behavior

A. V. Ivanov<sup>a,\*</sup>, O. V. Loseva<sup>a</sup>, T. A. Rodina<sup>b</sup>, and A. I. Smolentsev<sup>c,d</sup>

<sup>a</sup> Institute of Geology and Nature Management, Far East Branch, Russian Academy of Sciences, Blagoveshchensk, 675000 Russia

<sup>b</sup> Amur State University, Blagoveshchensk, 675027 Russia

<sup>c</sup> Nikolaev Institute of Inorganic Chemistry, Siberian Branch, Russian Academy of Sciences, Novosibirsk, 630090 Russia

<sup>d</sup> Novosibirsk State University, Novosibirsk, 630090 Russia

\*e-mail: alexander.v.ivanov@chemist.com

Received January 12, 2017

**Abstract**—Chemisorption of gold(III) from solutions in 2 M HCl with freshly precipitated binuclear zinc dithiocarbamate  $[\text{Zn}_2(\text{S}_2\text{CN}(\text{C}_4\text{H}_9)_2)_4]$  resulted in the formation of a polymeric heteronuclear gold(III)–zinc(II) dithiocarbamato-chlorido complex ( $[\text{Au}\{\text{S}_2\text{CN}(\text{C}_4\text{H}_9)_2\}_2]_2[\text{ZnCl}_4]_n$ ) (**I**), which was characterized by MAS  $^{13}\text{C}$  NMR, X-ray diffraction (CIF file CCDC no. 1526616), and simultaneous thermal analysis. Compound **I** isolated on a preparative scale was found to have a highly intricate supramolecular structure composed of 13 centrosymmetric and non-centrosymmetric isomeric complex cations,  $[\text{Au}\{\text{S}_2\text{CN}(\text{C}_4\text{H}_9)_2\}_2]^+$ , with 24 structurally non-equivalent BuDtc ligands, and six isomeric  $[\text{ZnCl}_4]^{2-}$  anions. The isomeric gold(III) cations perform different structural functions. Four and six cations are involved in the formation of two sorts of long-period cation–cationic chains (via pair non-valence secondary Au···S bonds):  $(\cdots\text{A}\cdots\text{B}\cdots\text{C}\cdots\text{D}\cdots\text{C}\cdots\text{B}\cdots)_n$  and  $(\cdots\text{F}\cdots\text{G}\cdots\text{H}\cdots\text{I}\cdots\text{J}\cdots\text{K}\cdots)_n$ . The discrete E, L, and M cations and the  $[\text{ZnCl}_4]^{2-}$  complex anions are located alongside of the polymer chains and do not take part in the secondary interactions. According to simultaneous thermal analysis, thermolysis of **I** includes destruction of the dithiocarbamate moiety with reduction of gold to the metal in the cation and liberation of zinc chloride with partial conversion to ZnS in the anion.

**Keywords:** zinc dialkyl dithiocarbamates, gold species extracted from solutions, heteronuclear gold(III)–zinc(II) dithiocarbamato-chlorido complexes, crystal and supramolecular structures, X-ray diffraction,  $^{13}\text{C}$  MAS NMR, simultaneous thermal analysis

**DOI:** 10.1134/S1070328417080036

## INTRODUCTION

Zinc dithiocarbamates, which are most often binuclear  $[\text{Zn}_2(\text{S}_2\text{CNR}_2)_4]$  and incorporate two bridging and two chelating ligands, offer a broad range of practical applications: in analytical chemistry [1], industry (rubber vulcanization) [2], agriculture (biocides) [3], and medicine (owing to antibacterial properties [4] and pharmacological activity towards glaucoma [5, 6] and diabetes mellitus [7]). Dithiocarbamate complexes are also used as precursors of nanocrystalline and film zinc sulfides, useful for their narrow bandgap (3.2–3.9 eV), in the semiconductor industry for manufacturing of solar cells, luminescent materials, and chemosensors [8–13].

In addition, freshly precipitated zinc dithiocarbamates are capable of effective chemisorption-based extraction of gold(III) from solutions to give heterometallic dithiocarbamato-chlorido complexes of the ionic type. Previously, we have prepared a series of heteronuclear gold(III)–zinc(II) complexes of various composition and structures, namely,  $[\text{Au}_2\{\text{S}_2\text{CN}(\text{CH}_3)_2\}_4][\text{ZnCl}_4]$ ,  $([\text{Au}\{\text{S}_2\text{CN}(\text{CH}_2)_4\text{O}\}_2]_2 \cdot [\text{ZnCl}_4] \cdot 2\text{H}_2\text{O})_n$ ,  $([\text{Au}\{\text{S}_2\text{CN}(\text{C}_2\text{H}_5)_2\}_2]_2[\text{ZnCl}_4] \cdot 1/2\text{C}_3\text{H}_6\text{O} \cdot 1/2\text{CHCl}_3)_n$ ,  $([\text{H}_3\text{O}][\text{Au}_3\{\text{S}_2\text{CN(iso-C}_3\text{H}_7)_2\}_6][\text{ZnCl}_4]_2 \cdot \text{H}_2\text{O})_n$ ,  $([\text{H}_3\text{O}][\text{Au}_2\{\text{S}_2\text{CN}(\text{CH}_2)_6\}_4][\text{Au}\{\text{S}_2\text{CN}(\text{CH}_2)_6\}_2][\text{ZnCl}_4]_2)_n$ , and  $([\text{NH}_2(\text{C}_4\text{H}_9)_2][\text{Au}\{\text{S}_2\text{CN}(\text{C}_4\text{H}_9)_2\}_2][\text{ZnCl}_4])_n$ , and have studied their structural organization and thermal behav-

ior by X-ray diffraction,  $^{13}\text{C}$  MAS NMR, and simultaneous thermal analysis (STA) [14–19]. The formation of the last-mentioned gold(III)–zinc(II)–dibutylammonium complex is associated with irreversible decomposition of some of the dibutyl dithiocarbamate groups on long-term contact of the chemisorbing complex with  $\text{AuCl}_3$  solutions of low concentration [19]. The intricately organized supramolecular structures of these complexes comprise mononuclear  $[\text{Au}(\text{S}_2\text{CNR}_2)_2]^+$ , binuclear  $[\text{Au}_2(\text{S}_2\text{CNR}_2)_4]^{2+}$ , and trinuclear  $[\text{Au}_3(\text{S}_2\text{CNR}_2)_6]^{3+}$  complex cations and various cation–cationic and cation–anionic polymer chains as structural units.

In this study, devoted to the chemisorption activity of freshly precipitated zinc dibutyl dithiocarbamate  $[\text{Zn}_2\{\text{S}_2\text{CN}(\text{C}_4\text{H}_9)_2\}_4]$  towards a solution of  $\text{H}[\text{AuCl}_4]$  (with  $\text{Au}^{3+}$  content of 4.15 mg/mL), the polymeric heteronuclear gold(III)–zinc(II)–dithiocarbamato-chlorido complex  $([\text{Au}\{\text{S}_2\text{CN}(\text{C}_4\text{H}_9)_2\}_2]_2[\text{ZnCl}_4])_n$  (**I**), characterized by multiple isomerization of the ionic structural units with an intricate supramolecular structure, was isolated as an individual gold(III) binding species. The structural organization and thermal behavior of **I** were studied by X-ray diffraction,  $^{13}\text{C}$  MAS NMR, and STA.

## EXPERIMENTAL

Sodium dibutyl dithiocarbamate was prepared by the reaction of carbon disulfide (Merck) with dibutylamine (Aldrich) in an alkaline medium [20] and the corresponding binuclear zinc complex was obtained by precipitation of  $\text{Zn}^{2+}$  ions from the aqueous phase with  $\text{Na}\{\text{S}_2\text{CN}(\text{C}_4\text{H}_9)_2\} \cdot \text{H}_2\text{O}$  taken in a stoichiometric ratio [21].<sup>1</sup> The starting compounds were identified using the  $^{13}\text{C}$  MAS NMR spectral data ( $\delta$ , ppm):

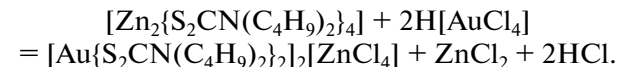
$\text{Na}\{\text{S}_2\text{CN}(\text{C}_4\text{H}_9)_2\} \cdot \text{H}_2\text{O}$ : 208.3 ( $-\text{S}_2\text{CN}=$ ), 55.2 ( $=\text{NCH}_2-$ ), 30.0, 21.0 ( $-\text{CH}_2-$ ), 15.6, 14.9, 14.5 (2 : 1 : 1,  $-\text{CH}_3$ ).

$[\text{Zn}_2\{\text{S}_2\text{CN}(\text{C}_4\text{H}_9)_2\}_4]$ : 203.4, 200.4 (34)\* (1 : 1,  $-\text{S}_2\text{CN}=$ ); 61.5, 58.6 (1 : 3,  $=\text{NCH}_2-$ ); 33.8, 32.9, 31.3, 30.0 (1 : 3 : 2 : 2,  $-\text{CH}_2-$ ); 16.2, 14.7, 14.5, 14.1 (1 : 1 : 1 : 1,  $-\text{CH}_3$ ) [21] (\*asymmetric  $^{13}\text{C}$ – $^{14}\text{N}$  doublet, Hz).

**Synthesis of I.** The preparation of the polymeric bis(*N,N*-dibutyl dithiocarbamato-*S,S*)gold(III) tetrachlorozincate (**I**) was based on the heterogeneous reaction of freshly precipitated zinc dibutyl dithiocarbamate with a solution of  $\text{H}[\text{AuCl}_4]$  in 2 M HCl,

<sup>1</sup> Apart from our publication [21], the structure of  $[\text{Zn}_2\{\text{S}_2\text{CN}(\text{C}_4\text{H}_9)_2\}_4]$  was reported somewhat later in [22]. Among the zinc dithiocarbamates structurally characterized by now [7–11, 21–37], the non-centrosymmetric dibutyl dithiocarbamate complex, like the dimethyl dithiocarbamate complex [23], is specially distinguished by stabilization of the central  $[\text{Zn}_2\text{S}_4\text{C}_2]$  tricyclic structural fragment in a distorted boat conformation.

which proceeded by the mechanism of chemisorption with partial ion exchange:



A solution of  $\text{AuCl}_3$  in 2 M HCl (10 mL) containing 41.5 mg of gold was added to freshly precipitated zinc dibutyl dithiocarbamate (100 mg), and the mixture was magnetically stirred for 1 h. The resulting homogeneous yellow-brown plastic paste was separated, covered with water, then thoroughly triturated many times to wash out water-soluble impurities, and dried on the filter. For X-ray diffraction experiment, the transparent yellow-orange square prismatic crystals of **I** were obtained from an acetone solution by slow evaporation of the solvent.

The identity of compound **I** was confirmed by  $^{13}\text{C}$  MAS NMR data ( $\delta$ , ppm):

$([\text{Au}\{\text{S}_2\text{CN}(\text{C}_4\text{H}_9)_2\}_2]_2[\text{ZnCl}_4])_n$ : 195.0, 194.7, 194.1 (~1 : 3 : 2,  $-\text{S}_2\text{CN}=$ ); 53.5, 52.6, 50.2, 49.9, 49.7, 49.6, 49.4, 48.7 ( $=\text{NCH}_2-$ ); 30.5, 29.8, 29.5, 29.4, 29.3, 29.1 ( $-\text{CH}_2-$ ); 21.1, 20.9, 20.7, 20.6, 20.4, 20.1 ( $-\text{CH}_2-$ ); 16.5, 15.7, 15.6, 15.1, 15.0, 14.4, 14.3 ( $-\text{CH}_3$ ).

$^{13}\text{C}$  MAS NMR spectra were recorded on a CMX-360 spectrometer (Agilent/Variian/Chemagnetics InfinityPlus) operating at 90.52 MHz with a superconducting magnet  $B_0 = 8.46$  T and Fourier transformation. The proton cross-polarization and  $^{13}\text{C}$ – $^1\text{H}$  decoupling with a radiofrequency field at a proton resonance frequency were used [38]. A ~80 mg sample of **I** was placed into 4.0 mm  $\text{ZrO}_2$  ceramic rotor. The  $^{13}\text{C}$  MAS NMR measurements were performed using magic angle spinning at 5300(1) Hz, 1100–1200 acquisitions, 4.9  $\mu\text{s}$  proton  $\pi/2$ -pulses, 2.5 ms  $^1\text{H}$ – $^{13}\text{C}$  contact time, and 3.0–5.0 s gap between the pulses. The isotropic  $^{13}\text{C}$  chemical shifts,  $\delta$  (ppm), were referred to a component of the external standard, crystalline adamantane ( $\delta = 38.48$  ppm relative to tetramethylsilane). The isotropic  $^{13}\text{C}$  chemical shifts were corrected for the magnetic field strength drift, the frequency equivalent of which is 0.051 Hz/h.

**X-ray diffraction analysis** was carried out on a Bruker-Nonius X8 Apex CCD diffractometer ( $\text{MoK}_\alpha$  radiation,  $\lambda = 0.71073$  Å, graphite monochromator) at 150(2) K. The data were collected by a standard procedure (narrow frame  $\varphi$ - and  $\omega$  scan mode). The absorption corrections were applied empirically (SADABS) [39]. The structure was solved by direct methods and refined by the least-squares method (on  $F^2$ ) in the full-matrix anisotropic approximation of non-hydrogen atoms. The positions of hydrogen atoms were calculated geometrically and included in the refinement in the riding model. In the disordered complex anion,  $[\text{ZnCl}_4]^{2-}$ , the *A* and *B* site occupancies by the randomly distributed Zn(4) and Cl(44) atoms were refined as 0.693(5) and 0.307(5), respectively. The

**Table 1.** Crystal data and X-ray experiment and structure refinement details for **I**

Parameter	Value
Empirical formula	C <sub>36</sub> H <sub>72</sub> N <sub>4</sub> S <sub>8</sub> Cl <sub>4</sub> ZnAu <sub>2</sub>
<i>M</i>	1418.56
System	Monoclinic
Space group	<i>C</i> 2/ <i>c</i>
<i>a</i> , Å	69.378(8)
<i>b</i> , Å	22.907(3)
<i>c</i> , Å	44.103(5)
β, deg	107.930(2)
<i>V</i> , Å <sup>3</sup>	66686(14)
<i>Z</i>	48
ρ(calcd.), g/cm <sup>3</sup>	1.696
μ, mm <sup>-1</sup>	6.216
<i>F</i> (000)	33600
Crystal size, mm	0.25 × 0.25 × 0.12
θ Range for data collection, deg	1.43–25.68
Ranges of reflection indices	−84 ≤ <i>h</i> ≤ 79, −14 ≤ <i>k</i> ≤ 27, −53 ≤ <i>l</i> ≤ 53
Number of measured reflections	196611
Number of unique reflections ( <i>R</i> <sub>int</sub> )	62 498 (0.0672)
Number of reflections with <i>I</i> > 2σ( <i>I</i> )	33547
Number of refinement parameters	3011
GOOF	1.068
<i>R</i> -factors on <i>F</i> <sup>2</sup> > 2σ( <i>F</i> <sup>2</sup> )	<i>R</i> <sub>1</sub> = 0.0729, <i>wR</i> <sub>2</sub> = 0.1665
<i>R</i> -factors (all reflections)	<i>R</i> <sub>1</sub> = 0.1620, <i>wR</i> <sub>2</sub> = 0.1916
Residual electron density (max/min), e/Å <sup>3</sup>	3.829/−3.270

data collection and editing and refinement of unit cell parameters were carried out using the APEX2 [39] and SAINT [39] program packages. The structure solution and refinement calculations were carried out using the SHELXTL program package [39]. Selected crystallographic data and structure refinement details for **I** are summarized in Table 1 and bond lengths and angles are in Table 2.

Atom coordinates and bond lengths and angles are deposited with the Cambridge Crystallographic Data Centre (no. 1526616; <http://www.ccdc.cam.ac.uk/conts/retrieving.html>).

The thermal properties of **I** were studied by STA including simultaneous recording of the thermogravimetric (TG) and differential scanning calorimetry (DSC) curves. The study was carried out on an STA 449C Jupiter instrument (NETZSCH) in corundum crucibles with a hole in the lid for maintaining the 1 atm vapor pressure during the thermal decomposition of the sample. Heating was conducted up to 1100°C under argon at a 5°C/min rate. For better identification of thermal effects in the low-temperature region, the measurements were additionally con-

ducted in aluminum crucibles. The sample weight was 2.166–7.184 mg. The temperature and the weight changes were determined to ±0.8°C and ±1 × 10<sup>−4</sup> mg accuracy, respectively. The TG and DSC curves were measured using the correction file and the temperature and sensitivity calibrations for the specified temperature program and heating rate. An alternative determination of the melting points of the complex was performed on a PTP(M) instrument (OJSC Khimlaborpribor).

## RESULTS AND DISCUSSION

The reaction of freshly precipitated zinc dibutyl dithiocarbamate [Zn<sub>2</sub>{S<sub>2</sub>CN(C<sub>4</sub>H<sub>9</sub>)<sub>2</sub>}<sub>4</sub>] (finely crystalline white precipitate) with a solution of AuCl<sub>3</sub> is accompanied by the gradual change in the precipitate color to yellow-brown (with the solution being completely decolorized) and coarsening of the precipitate particles followed by agglomeration into a uniform plastic paste. These changes attest to the formation of new compounds in the system.

**Table 2.** Selected bond lengths ( $d$ ), bond angles ( $\omega$ ), and torsion angles ( $\phi$ ) in I\*

Bond	$d, \text{\AA}$	Bond	$d, \text{\AA}$
Cations			
Au(1)–S(11)	2.332(3)	S(11)–C(1)	1.745(14)
Au(1)–S(12)	2.335(4)	S(12)–C(1)	1.699(14)
Au(1)···S(23)	3.656(3)	N(1)–C(1)	1.297(15)
Au(2)–S(21)	2.340(3)	S(21)–C(10)	1.692(12)
Au(2)–S(22)	2.336(3)	S(22)–C(10)	1.756(13)
Au(2)–S(23)	2.327(3)	S(23)–C(19)	1.707(11)
Au(2)–S(24)	2.325(3)	S(24)–C(19)	1.711(13)
Au(2)···S(11)	3.462(4)	N(2)–C(10)	1.323(15)
Au(2)···S(32)	3.601(3)	N(3)–C(19)	1.311(14)
Au(3)–S(31)	2.331(3)	S(31)–C(28)	1.745(15)
Au(3)–S(32)	2.335(4)	S(32)–C(28)	1.731(15)
Au(3)–S(33)	2.327(4)	S(33)–C(37)	1.735(15)
Au(3)–S(34)	2.330(4)	S(34)–C(37)	1.724(15)
Au(3)···S(22)	3.781(3)	N(4)–C(28)	1.310(18)
Au(3)···S(42)	3.720(4)	N(5)–C(37)	1.290(18)
Au(4)–S(41)	2.315(4)	S(41)–C(46)	1.744(16)
Au(4)–S(42)	2.343(4)	S(42)–C(46)	1.713(15)
Au(4)···S(34)	3.946(4)	N(6)–C(46)	1.313(15)
Au(5)–S(51)	2.332(4)	S(52)–C(55)	1.718(15)
Au(5)–S(52)	2.334(4)	S(53)–C(64)	1.661(16)
Au(5)–S(53)	2.255(5)	S(54)–C(64)	1.765(15)
Au(5)–S(54)	2.278(6)	N(7)–C(55)	1.352(17)
S(51)–C(55)	1.680(17)	N(8)–C(64)	1.318(17)
Au(6)–S(61)	2.317(4)	S(61)–C(73)	1.705(14)
Au(6)–S(62)	2.344(3)	S(62)–C(73)	1.712(15)
Au(6)–S(63)	2.323(4)	S(63)–C(82)	1.729(14)
Au(6)–S(64)	2.331(3)	S(64)–C(82)	1.710(14)
Au(6)···S(71)	3.829(3)	N(9)–C(73)	1.371(17)
Au(6)···S(113) <sup>c</sup>	3.531(4)	N(10)–C(82)	1.323(16)
Au(7)–S(71)	2.336(3)	S(71)–C(91)	1.731(12)
Au(7)–S(72)	2.338(3)	S(72)–C(91)	1.729(12)
Au(7)–S(73)	2.333(3)	S(73)–C(100)	1.739(14)
Au(7)–S(74)	2.332(3)	S(74)–C(100)	1.723(14)
Au(7)···S(63)	3.576(4)	N(11)–C(91)	1.288(14)
Au(7)···S(84)	3.590(4)	N(12)–C(100)	1.308(16)
Au(8)–S(81)	2.336(4)	S(81)–C(109)	1.719(13)
Au(8)–S(82)	2.327(4)	S(82)–C(109)	1.742(13)
Au(8)–S(83)	2.343(5)	S(83)–C(118)	1.65(2)
Au(8)–S(84)	2.311(4)	S(84)–C(118)	1.745(17)
Au(8)···S(74)	3.808(4)	N(13)–C(109)	1.298(14)
Au(8)···S(92)	3.628(4)	N(14)–C(118)	1.37(2)
Au(9)–S(91)	2.318(3)	S(91)–C(127)	1.698(14)
Au(9)–S(92)	2.330(3)	S(92)–C(127)	1.749(14)

**Table 2.** (Contd.)

Bond	<i>d</i> , Å	Bond	<i>d</i> , Å
Cations			
Au(9)–S(93)	2.346(3)	S(93)–C(136)	1.717(13)
Au(9)–S(94)	2.334(3)	S(94)–C(136)	1.740(13)
Au(9)···S(82)	3.552(4)	N(15)–C(127)	1.313(16)
Au(9)···S(101)	3.619(4)	N(16)–C(136)	1.312(15)
Au(10)–S(101)	2.326(4)	S(101)–C(145)	1.73(2)
Au(10)–S(102)	2.322(4)	S(102)–C(145)	1.700(16)
Au(10)–S(103)	2.322(4)	S(103)–C(154)	1.744(15)
Au(10)–S(104)	2.330(4)	S(104)–C(154)	1.729(18)
Au(10)···S(93)	3.822(4)	N(17)–C(145)	1.30(2)
Au(10)···S(111)	3.462(4)	N(18)–C(154)	1.30(2)
Au(11)–S(111)	2.332(5)	S(111)–C(163)	1.727(16)
Au(11)–S(112)	2.327(4)	S(112)–C(163)	1.682(18)
Au(11)–S(113)	2.329(4)	S(113)–C(172)	1.726(16)
Au(11)–S(114)	2.333(4)	S(114)–C(172)	1.722(17)
Au(11)···S(61) <sup>d</sup>	3.576(5)	N(19)–C(163)	1.33(2)
Au(11)···S(103)	3.713(4)	N(20)–C(172)	1.309(18)
Au(12)–S(121)	2.331(4)	S(122)–C(181)	1.716(17)
Au(12)–S(122)	2.331(4)	S(123)–C(190)	1.711(14)
Au(12)–S(123)	2.326(3)	S(124)–C(190)	1.719(14)
Au(12)–S(124)	2.315(4)	N(21)–C(181)	1.297(18)
S(121)–C(181)	1.721(16)	N(22)–C(190)	1.329(16)
Au(13)–S(131)	2.331(4)	S(132)–C(199)	1.698(17)
Au(13)–S(132)	2.322(4)	S(133)–C(208)	1.698(16)
Au(13)–S(133)	2.333(4)	S(134)–C(208)	1.744(14)
Au(13)–S(134)	2.341(4)	N(23)–C(199)	1.300(18)
S(131)–C(199)	1.743(17)	N(24)–C(208)	1.314(16)
Anions			
Zn(1)–Cl(11)	2.258(4)	Zn(1)–Cl(13)	2.264(5)
Zn(1)–Cl(12)	2.283(4)	Zn(1)–Cl(14)	2.257(4)
Zn(2)–Cl(21)	2.239(5)	Zn(2)–Cl(23)	2.273(4)
Zn(2)–Cl(22)	2.273(4)	Zn(2)–Cl(24)	2.264(4)
Zn(3)–Cl(31)	2.257(6)	Zn(3)–Cl(33)	2.234(6)
Zn(3)–Cl(32)	2.262(5)	Zn(3)–Cl(34)	2.222(7)
Zn(4A)–Cl(41)	2.301(7)	Zn(4B)–Cl(41)	2.219(9)
Zn(4A)–Cl(42)	2.270(4)	Zn(4B)–Cl(42)	2.310(7)
Zn(4A)–Cl(43)	2.164(7)	Zn(4B)–Cl(43)	2.454(9)
Zn(4A)–Cl(44A)	2.274(8)	Zn(4B)–Cl(44B)	2.183(16)
Zn(5)–Cl(51)	2.281(4)	Zn(5)–Cl(53)	2.255(5)
Zn(5)–Cl(52)	2.264(4)	Zn(5)–Cl(54)	2.278(6)
Zn(6)–Cl(61)	2.258(5)	Zn(6)–Cl(63)	2.267(6)
Zn(6)–Cl(62)	2.279(5)	Zn(6)–Cl(64)	2.252(4)

**Table 2.** (Contd.)

Angle	$\omega$ , deg	Angle	$\omega$ , deg
Cations			
S(11)Au(1)S(12)	74.72(13)	Au(1)S(12)C(1)	87.6(5)
S(11)Au(1)S(12) <sup>a</sup>	105.28(13)	S(11)C(1)S(12)	110.6(7)
Au(1)S(11)C(1)	86.6(5)		
S(21)Au(2)S(22)	75.78(11)	Au(2)S(21)C(10)	86.4(4)
S(21)Au(2)S(23)	178.92(12)	Au(2)S(22)C(10)	85.1(4)
S(21)Au(2)S(24)	104.13(12)	Au(2)S(23)C(19)	85.8(4)
S(22)Au(2)S(23)	104.67(11)	Au(2)S(24)C(19)	85.8(4)
S(22)Au(2)S(24)	177.27(12)	S(21)C(10)S(22)	112.8(7)
S(23)Au(2)S(24)	75.47(11)	S(23)C(19)S(24)	112.8(7)
S(31)Au(3)S(32)	75.60(14)	Au(3)S(31)C(28)	86.7(5)
S(31)Au(3)S(33)	174.54(14)	Au(3)S(32)C(28)	86.8(5)
S(31)Au(3)S(34)	104.29(14)	Au(3)S(33)C(37)	86.0(5)
S(32)Au(3)S(33)	104.30(15)	Au(3)S(34)C(37)	86.2(5)
S(32)Au(3)S(34)	178.68(14)	S(31)C(28)S(32)	110.7(9)
S(33)Au(3)S(34)	75.68(15)	S(33)C(37)S(34)	111.3(9)
S(41)Au(4)S(42)	75.09(15)	Au(4)S(42)C(46)	87.0(5)
S(41)Au(4)S(42) <sup>b</sup>	104.91(15)	S(41)C(46)S(42)	110.4(7)
Au(4)S(41)C(46)	87.2(5)		
S(51)Au(5)S(52)	75.47(15)	Au(5)S(51)C(55)	85.5(5)
S(51)Au(5)S(53)	176.82(16)	Au(5)S(52)C(55)	84.6(5)
S(51)Au(5)S(54)	104.70(14)	Au(5)S(53)C(64)	87.1(5)
S(52)Au(5)S(53)	104.26(15)	Au(5)S(54)C(64)	84.5(5)
S(52)Au(5)S(54)	178.34(15)	S(51)C(55)S(52)	114.4(8)
S(53)Au(5)S(54)	75.67(15)	S(53)C(64)S(54)	112.7(7)
S(61)Au(6)S(62)	74.97(14)	Au(6)S(61)C(73)	86.7(5)
S(61)Au(6)S(63)	176.70(16)	Au(6)S(62)C(73)	85.7(5)
S(61)Au(6)S(64)	103.09(15)	Au(6)S(63)C(82)	85.4(4)
S(62)Au(6)S(63)	105.70(13)	Au(6)S(64)C(82)	85.6(4)
S(62)Au(6)S(64)	174.87(14)	S(61)C(73)S(62)	112.2(7)
S(63)Au(6)S(64)	75.96(14)	S(63)C(82)S(64)	112.7(6)
S(71)Au(7)S(72)	75.64(11)	Au(7)S(71)C(91)	86.2(4)
S(71)Au(7)S(73)	177.03(13)	Au(7)S(72)C(91)	86.2(4)
S(71)Au(7)S(74)	104.45(11)	Au(7)S(73)C(100)	86.8(5)
S(72)Au(7)S(73)	104.68(11)	Au(7)S(74)C(100)	87.2(5)
S(72)Au(7)S(74)	179.19(13)	S(71)C(91)S(72)	111.9(7)
S(73)Au(7)S(74)	75.28(12)	S(73)C(100)S(74)	110.8(8)
S(81)Au(8)S(82)	75.02(13)	Au(8)S(81)C(109)	87.2(4)
S(81)Au(8)S(83)	178.01(17)	Au(8)S(82)C(109)	87.0(4)
S(81)Au(8)S(84)	105.96(16)	Au(8)S(83)C(118)	85.7(5)
S(82)Au(8)S(83)	103.65(17)	Au(8)S(84)C(118)	84.7(6)
S(82)Au(8)S(84)	178.38(16)	S(81)C(109)S(82)	110.3(7)
S(83)Au(8)S(84)	75.4(2)	S(83)C(118)S(84)	113.8(8)
S(91)Au(9)S(92)	75.90(12)	Au(9)S(91)C(127)	86.8(5)
S(91)Au(9)S(93)	176.74(13)	Au(9)S(92)C(127)	85.3(5)
S(91)Au(9)S(94)	103.37(12)	Au(9)S(93)C(136)	86.5(4)
S(92)Au(9)S(93)	105.37(11)	Au(9)S(94)C(136)	86.3(4)
S(92)Au(9)S(94)	179.09(13)	S(91)C(127)S(92)	112.0(7)
S(93)Au(9)S(94)	75.39(11)	S(93)C(136)S(94)	111.8(7)

**Table 2.** (Contd.)

Angle	$\omega$ , deg	Angle	$\omega$ , deg
Cations			
S(101)Au(10)S(102)	75.11(18)	Au(10)S(101)C(145)	86.3(5)
S(101)Au(10)S(103)	179.87(18)	Au(10)S(102)C(145)	87.3(6)
S(101)Au(10)S(104)	104.8(2)	Au(10)S(103)C(154)	87.3(6)
S(102)Au(10)S(103)	104.82(15)	Au(10)S(104)C(154)	87.3(6)
S(102)Au(10)S(104)	174.22(15)	S(101)C(145)S(102)	111.1(8)
S(103)Au(10)S(104)	75.30(16)	S(103)C(154)S(104)	109.8(10)
S(111)Au(11)S(112)	74.58(16)	Au(11)S(111)C(163)	86.1(6)
S(111)Au(11)S(113)	178.94(15)	Au(11)S(112)C(163)	87.3(6)
S(111)Au(11)S(114)	105.15(16)	Au(11)S(113)C(172)	87.6(5)
S(112)Au(11)S(113)	105.85(17)	Au(11)S(114)C(172)	87.6(5)
S(112)Au(11)S(114)	178.99(18)	S(111)C(163)S(112)	111.8(9)
S(113)Au(11)S(114)	74.44(16)	S(113)C(172)S(114)	109.8(8)
S(121)Au(12)S(122)	75.09(15)	Au(12)S(121)C(181)	86.6(5)
S(121)Au(12)S(123)	178.69(15)	Au(12)S(122)C(181)	86.7(5)
S(121)Au(12)S(124)	103.94(15)	Au(12)S(123)C(190)	85.8(5)
S(122)Au(12)S(123)	105.21(13)	Au(12)S(124)C(190)	86.0(5)
S(122)Au(12)S(124)	178.94(15)	S(121)C(181)S(122)	111.5(8)
S(123)Au(12)S(124)	75.76(13)	S(123)C(190)S(124)	112.4(8)
S(131)Au(13)S(132)	75.91(17)	Au(13)S(131)C(199)	85.1(5)
S(131)Au(13)S(133)	178.58(18)	Au(13)S(132)C(199)	86.4(5)
S(131)Au(13)S(134)	105.53(16)	Au(13)S(133)C(208)	86.6(5)
S(132)Au(13)S(133)	103.08(16)	Au(13)S(134)C(208)	85.3(5)
S(132)Au(13)S(134)	176.58(16)	S(131)C(199)S(132)	112.6(8)
S(133)Au(13)S(134)	75.53(13)	S(133)C(208)S(134)	112.5(8)
Anions			
Cl(11)Zn(1)Cl(12)	114.96(15)	Cl(12)Zn(1)Cl(13)	109.24(18)
Cl(11)Zn(1)Cl(13)	108.6(2)	Cl(12)Zn(1)Cl(14)	106.18(15)
Cl(11)Zn(1)Cl(14)	105.55(17)	Cl(13)Zn(1)Cl(14)	112.33(16)
Cl(21)Zn(2)Cl(22)	107.4(2)	Cl(22)Zn(2)Cl(23)	112.3(2)
Cl(21)Zn(2)Cl(23)	111.0(2)	Cl(22)Zn(2)Cl(24)	107.90(17)
Cl(21)Zn(2)Cl(24)	111.4(2)	Cl(23)Zn(2)Cl(24)	106.82(16)
Cl(31)Zn(3)Cl(32)	107.0(2)	Cl(32)Zn(3)Cl(33)	109.8(3)
Cl(31)Zn(3)Cl(33)	112.5(2)	Cl(32)Zn(3)Cl(34)	110.8(3)
Cl(31)Zn(3)Cl(34)	110.9(3)	Cl(33)Zn(3)Cl(34)	105.8(2)
Cl(41)Zn(4A)Cl(42)	110.8(2)	Cl(41)Zn(4B)Cl(42)	120.6(4)
Cl(41)Zn(4A)Cl(43)	115.5(3)	Cl(41)Zn(4B)Cl(43)	114.9(3)
Cl(41)Zn(4A)Cl(44A)	105.3(3)	Cl(41)Zn(4B)Cl(44B)	101.7(5)
Cl(42)Zn(4A)Cl(43)	112.7(2)	Cl(42)Zn(4B)Cl(43)	101.6(3)
Cl(42)Zn(4A)Cl(44A)	110.8(2)	Cl(42)Zn(4B)Cl(44B)	114.1(4)
Cl(43)Zn(4A)Cl(44A)	101.0(3)	Cl(43)Zn(4B)Cl(44B)	103.1(4)
Cl(51)Zn(5)Cl(52)	106.23(16)	Cl(52)Zn(5)Cl(53)	108.2(2)
Cl(51)Zn(5)Cl(53)	114.04(17)	Cl(52)Zn(5)Cl(54)	111.97(16)
Cl(51)Zn(5)Cl(54)	109.5(2)	Cl(53)Zn(5)Cl(54)	107.0(2)
Cl(61)Zn(6)Cl(62)	114.46(18)	Cl(62)Zn(6)Cl(63)	107.4(2)
Cl(61)Zn(6)Cl(63)	112.3(2)	Cl(62)Zn(6)Cl(64)	106.46(18)
Cl(61)Zn(6)Cl(64)	104.77(18)	Cl(63)Zn(6)Cl(64)	111.3(2)

Table 2. (Contd.)

Angle	$\phi$ , deg	Angle	$\phi$ , deg
Au(1)S(11)S(12)C(1) S(11)Au(1)C(1)S(12) S(11)C(1)N(1)C(2)	-172.7(8) -173.4(7) 5.6(18)	S(11)C(1)N(1)C(6) S(12)C(1)N(1)C(2) S(12)C(1)N(1)C(6)	172.4(10) -172.9(10) -6(2)
Au(2)S(21)S(22)C(10) Au(2)S(23)S(24)C(19) S(21)Au(2)C(10)S(22) S(23)Au(2)C(19)S(24) S(21)C(10)N(2)C(11) S(21)C(10)N(2)C(15)	178.8(8) 176.8(8) 179.0(7) 177.2(7) 1.5(17) -173.7(9)	S(22)C(10)N(2)C(11) S(22)C(10)N(2)C(15) S(23)C(19)N(3)C(20) S(23)C(19)N(3)C(24) S(24)C(19)N(3)C(20) S(24)C(19)N(3)C(24)	180.0(9) 4.8(16) 1.2(18) -177.8(11) -178.3(10) 2.7(18)
Au(3)S(31)S(32)C(28) Au(3)S(33)S(34)C(37) S(31)Au(3)C(28)S(32) S(33)Au(3)C(37)S(34) S(31)C(28)N(4)C(29) S(31)C(28)N(4)C(33)	-175.6(8) -170.2(8) -176.1(7) -171.3(7) -6(2) 178.0(12)	S(32)C(28)N(4)C(29) S(32)C(28)N(4)C(33) S(33)C(37)N(5)C(38) S(33)C(37)N(5)C(42) S(34)C(37)N(5)C(38) S(34)C(37)N(5)C(42)	173.7(12) -2(2) 3(3) -175.8(14) 179.9(14) 1(2)
Au(4)S(41)S(42)C(46) S(41)Au(4)C(46)S(42) S(41)C(46)N(6)C(47)	-174.4(8) -174.9(7) 0(2)	S(41)C(46)N(6)C(51) S(42)C(46)N(6)C(47) S(42)C(46)N(6)C(51)	177.8(12) -176.4(13) 1(2)
Au(5)S(51)S(52)C(55) Au(5)S(53)S(54)C(64) S(51)Au(5)C(55)S(52) S(53)Au(5)C(64)S(54) S(51)C(55)N(7)C(56) S(51)C(55)N(7)C(60)	178.7(9) 176.4(9) 178.9(8) 176.8(8) -6(2) 177.3(13)	S(52)C(55)N(7)C(56) S(52)C(55)N(7)C(60) S(53)C(64)N(8)C(65) S(53)C(64)N(8)C(69) S(54)C(64)N(8)C(65) S(54)C(64)N(8)C(69)	179.2(13) 2(2) -2(2) -164.0(16) 176.7(12) 14(2)
Au(6)S(61)S(62)C(73) Au(6)S(63)S(64)C(82) S(61)Au(6)C(73)S(62) S(63)Au(6)C(82)S(64) S(61)C(73)N(9)C(74) S(61)C(73)N(9)C(78)	-172.4(9) -173.4(8) -173.3(8) -174.3(7) 16(2) 179.8(10)	S(62)C(73)N(9)C(74) S(62)C(73)N(9)C(78) S(63)C(82)N(10)C(83) S(63)C(82)N(10)C(87) S(64)C(82)N(10)C(83) S(64)C(82)N(10)C(87)	-163.2(13) 0(2) -2(2) -178.7(10) 178.1(12) 1(2)
Au(7)S(71)S(72)C(91) Au(7)S(73)S(74)C(100) S(71)Au(7)C(91)S(72) S(73)Au(7)C(100)S(74) S(71)C(91)N(11)C(92) S(71)C(91)N(11)C(96)	178.6(8) 177.7(8) 178.8(7) 177.9(7) -5.3(16) 178.1(9)	S(72)C(91)N(11)C(92) S(72)C(91)N(11)C(96) S(73)C(100)N(12)C(101) S(73)C(100)N(12)C(105) S(74)C(100)N(12)C(101) S(74)C(100)N(12)C(105)	175.0(9) -1.6(17) -3(2) -179.6(10) 173.7(11) -3(2)
Au(8)S(81)S(82)C(109) Au(8)S(83)S(84)C(118) S(81)Au(8)C(109)S(82) S(83)Au(8)C(118)S(84) S(81)C(109)N(13)C(110) S(81)C(109)N(13)C(114)	171.7(8) -172.1(10) 172.5(7) -173.2(9) -8(2) -177.7(10)	S(82)C(109)N(13)C(110) S(82)C(109)N(13)C(114) S(83)C(118)N(14)C(119) S(83)C(118)N(14)C(123) S(84)C(118)N(14)C(119) S(84)C(118)N(14)C(123)	171.1(10) 1.0(18) 10(2) 174.0(12) -171.0(13) -7(2)
Au(9)S(91)S(92)C(127) Au(9)S(93)S(94)C(136) S(91)Au(9)C(127)S(92) S(93)Au(9)C(136)S(94) S(91)C(127)N(15)C(128) S(91)C(127)N(15)C(132)	-177.6(8) -177.7(8) -177.9(7) -178.0(7) 1(2) 179.5(14)	S(92)C(127)N(15)C(128) S(92)C(127)N(15)C(132) S(93)C(136)N(16)C(137) S(93)C(136)N(16)C(141) S(94)C(136)N(16)C(137) S(94)C(136)N(16)C(141)	-178.8(12) 0(2) 2(2) 174.3(11) -177.9(10) -6(2)

**Table 2.** (Contd.)

Angle	$\phi$ , deg	Angle	$\phi$ , deg
Au(10)S(101)S(102)C(145)	175.6(10)	S(102)C(145)N(17)C(146)	178.2(14)
Au(10)S(103)S(104)C(154)	173.8(9)	S(102)C(145)N(17)C(150)	-2(3)
S(101)Au(10)C(145)S(102)	176.1(9)	S(103)C(154)N(18)C(155)	9(2)
S(103)Au(10)C(154)S(104)	174.4(9)	S(103)C(154)N(18)C(159)	-176.0(14)
S(101)C(145)N(17)C(146)	-4(3)	S(104)C(154)N(18)C(155)	-171.1(14)
S(101)C(145)N(17)C(150)	175.8(14)	S(104)C(154)N(18)C(159)	4(3)
Au(11)S(111)S(112)C(163)	174.3(10)	S(112)C(163)N(19)C(164)	175.8(14)
Au(11)S(113)S(114)C(172)	-171.6(9)	S(112)C(163)N(19)C(168)	7(2)
S(111)Au(11)C(163)S(112)	174.9(9)	S(113)C(172)N(20)C(173)	4(2)
S(113)Au(11)C(172)S(114)	-172.3(8)	S(113)C(172)N(20)C(177)	-177.0(12)
S(111)C(163)N(19)C(164)	0(2)	S(114)C(172)N(20)C(173)	-174.1(12)
S(111)C(163)N(19)C(168)	-168.3(13)	S(114)C(172)N(20)C(177)	5(2)
Au(12)S(121)S(122)C(181)	177.7(10)	S(122)C(181)N(21)C(182)	-164.9(16)
Au(12)S(123)S(124)C(190)	-178.2(8)	S(122)C(181)N(21)C(186)	4(3)
S(121)Au(12)C(181)S(122)	177.9(9)	S(123)C(190)N(22)C(191)	7(2)
S(123)Au(12)C(190)S(124)	-178.4(7)	S(123)C(190)N(22)C(195)	-169.3(11)
S(121)C(181)N(21)C(182)	15(3)	S(124)C(190)N(22)C(191)	-176.4(11)
S(121)C(181)N(21)C(186)	-176.6(15)	S(124)C(190)N(22)C(195)	7(2)
Au(13)S(131)S(132)C(199)	-176.9(10)	S(132)C(199)N(23)C(200)	-166.6(17)
Au(13)S(133)S(134)C(208)	179.7(9)	S(132)C(199)N(23)C(204)	-10(2)
S(131)Au(13)C(199)S(132)	-177.3(9)	S(133)C(208)N(24)C(209)	1(2)
S(133)Au(13)C(208)S(134)	179.7(8)	S(133)C(208)N(24)C(213)	178.7(11)
S(131)C(199)N(23)C(200)	15(3)	S(134)C(208)N(24)C(209)	-178.8(12)
S(131)C(199)N(23)C(204)	172.0(14)	S(134)C(208)N(24)C(213)	-1(2)

\* Symmetry codes: <sup>a</sup> -x, -y, -z; <sup>b</sup> -x, 1-y, -z; <sup>c</sup> x, y-1, z; <sup>d</sup> x, 1+y, z.

In the <sup>13</sup>C MAS NMR spectrum of a polycrystalline sample of **I** (Fig. 1), the structural states of the BuDtc ligand carbon atoms (=NC(S)S-, =NCH<sub>2</sub>-, -CH<sub>2</sub>-, -CH<sub>3</sub>) give rise to multicomponent groups of resonance signals (see the section Synthesis), which reflects the multiple structural non-equivalence of the dithio ligands in the complex. The mathematical modeling of the asymmetric <sup>13</sup>C signal of the =NC(S)S- groups provides more definite conclusion that the poorly resolved internal structure of the spectrum is caused by superposition of three resonance signals in an integrated intensity ratio of about 1 : 3 : 2. This indicates that complex **I** has six (or a number divisible by 6) structurally non-equivalent BuDtc ligands. The markedly lower  $\delta(^{13}\text{C})$  chemical shifts of all =NC(S)S- groups in **I** in comparison with the initial zinc complex reflect the increasing electron shielding of carbon nuclei, caused by complete redistribution of the BuDtc ligands between the zinc and gold coordination spheres. (Thus, in the covalent

binding of the BuDtc ligands by gold(III), the electronic system of gold participates more efficiently in the additional shielding of the carbon nuclei of the =NC(S)S- groups). The foregoing attests to a complex structural organization of the new heteronuclear gold(III)-zinc(II) complex, the supramolecular self-organization of which was established by X-ray crystallography.

The unit cell of complex **I** includes 48 formula units [Au{S<sub>2</sub>CN(C<sub>4</sub>H<sub>9</sub>)<sub>2</sub>}<sub>2</sub>][ZnCl<sub>4</sub>] (Fig. 2). The ionic structural units are represented by thirteen non-equivalent complex cations [Au{S<sub>2</sub>CN(C<sub>4</sub>H<sub>9</sub>)<sub>2</sub>}<sub>2</sub>]<sup>+</sup> (below referred to as cations A–M with the Au(1)–Au(13) atoms, respectively) and six [ZnCl<sub>4</sub>]<sup>2-</sup> anions. Most of gold(III) cations, except for A with Au(1) and D with Au(4), are non-centrosymmetric and include pairs of non-equivalent ligands. Thus, compound **I** includes altogether 24 structurally non-equivalent BuDtc ligands, which is consistent with the above <sup>13</sup>C MAS NMR data. In all [Au{S<sub>2</sub>CN(C<sub>4</sub>H<sub>9</sub>)<sub>2</sub>}<sub>2</sub>]<sup>+</sup> cations, the

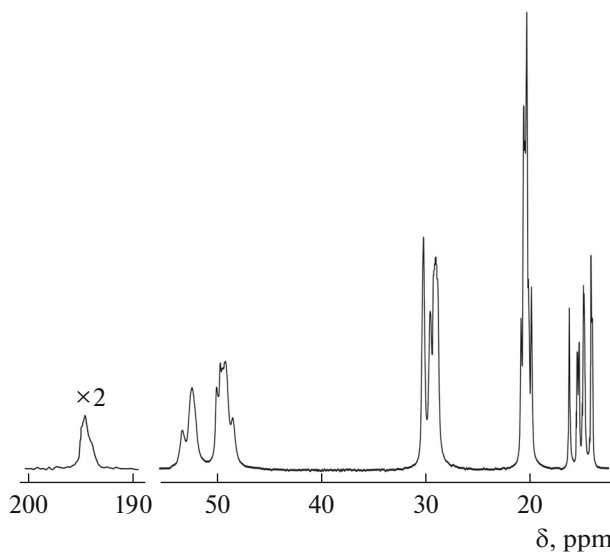


**Fig. 1.**  $^{13}\text{C}$  MAS NMR spectrum of complex **I**. Number of acquisitions/spinning frequency: 1160/5.3 kHz.

chelating BuDtc ligands are coordinated in an approximately *S,S'*-anisobidentate fashion (Fig. 3), with the Au—S bond length being in the 2.315–2.346 Å range (Table 2). The only exception is one of the ligands of cation E with a reliably higher binding strength: Au(5)—S(53), 2.255; Au(5)—S(54), 2.278 Å.

In each cation, the *S,S'*-bidentate terminal coordination of the BuDtc ligands gives rise to the central bicyclic  $[\text{CS}_2\text{AuS}_2\text{C}]$  fragment in which the interatomic distances in the small four-membered  $[\text{AuS}_2\text{C}]$  rings (Au···C, 2.763–2.840; S···S, 2.820–2.872 Å) are much shorter than the sum of the van der Waals radii of the corresponding pairs of atoms (3.36 and 3.60 Å) [40–42]. The considerably proximate positions of the

opposing gold and carbon atoms are indicative of *trans*-annular interaction between them and reflect high  $\pi$ -electron density within the rings. The deviation of the AuSSC ( $170.2^\circ$ – $179.7^\circ$ ) and SAuCS torsion angles ( $171.3^\circ$ – $179.7^\circ$ ) from  $180^\circ$  is associated with some tetrahedral distortion of the essentially planar  $[\text{AuS}_2\text{C}]$  rings, which can be described as ring folding along the S–S axis. In the  $[\text{AuS}_4]$  chromophores, the environment of gold atoms is approximately square (the diagonal SAuS angles are in the  $174.22^\circ$ – $180^\circ$  range), which corresponds to the low-spin (intraorbital)  $dsp^2$ -hybrid state of the central gold atom. In the  $\text{C}_2\text{NCS}_2$  fragments of the BuDtc ligands, the atoms are not strictly coplanar either, as indicated by the SCNC torsion angles differing from  $180^\circ$  or  $0^\circ$  (Table 2). The greater strength of the N—C(S)S bonds (1.288–1.371 Å) compared with the N—CH<sub>2</sub> bonds (1.418–1.504 Å) is due to admixing of the  $sp^2$ - to  $sp^3$ -hybrid state of carbon and nitrogen atoms, which defines a contribution of double bonding to this formally single bond as a result of mesomeric effect.

The anionic part of structure **I** is composed of six non-equivalent  $[\text{ZnCl}_4]^{2-}$  anions shaped as distorted tetrahedra (ClZnCl angles of  $104.77^\circ$ – $114.96^\circ$  noticeably deviate from an ideal tetrahedral value) with the  $sp^3$ -hybrid state of the central zinc atom (Fig. 4). In one anion, the Zn(4) and Cl(44) atoms are statistically distributed between *A* and *B* sites with occupancies of 0.693(5) and 0.307(5). The Cl atoms in all anions are non-equivalent, the Zn—Cl bond lengths (2.222–2.283 Å) being consistent with the data of [43, 44]. In the disordered Zn(4) anion, the scatter in the Zn—Cl bond lengths and ClZnCl angles is more pronounced: 2.164–2.454 Å and  $101.0^\circ$ – $120.6^\circ$ . The type of structural differences between non-equivalent  $[\text{Au}\{\text{S}_2\text{CN}(\text{C}_4\text{H}_9)_2\}_2]^+$  complex cations and  $[\text{ZnCl}_4]^{2-}$

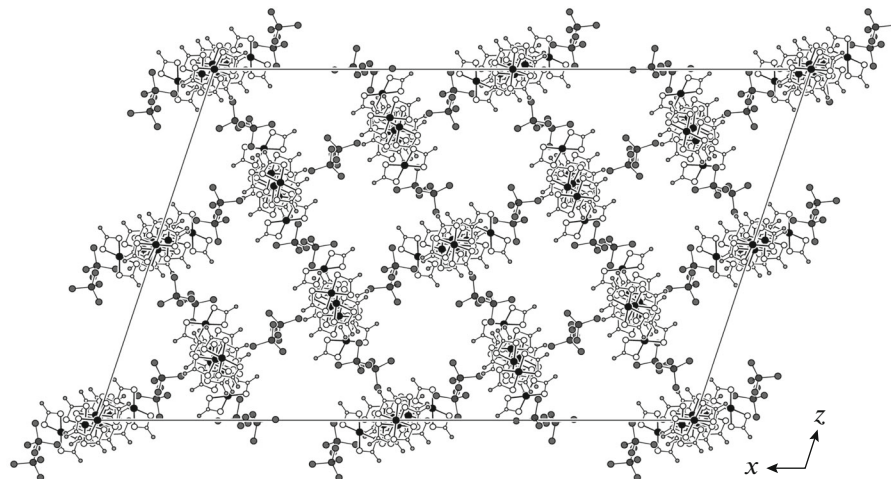


**Fig. 2.** Projection of the structure of  $([\text{Au}\{\text{S}_2\text{CN}(\text{C}_4\text{H}_9)_2\}_2]^+)_2[\text{ZnCl}_4]_n$  (**I**) on the  $xz$  plane. The alkyl substituents of the dithiocarbamate ligands are omitted.

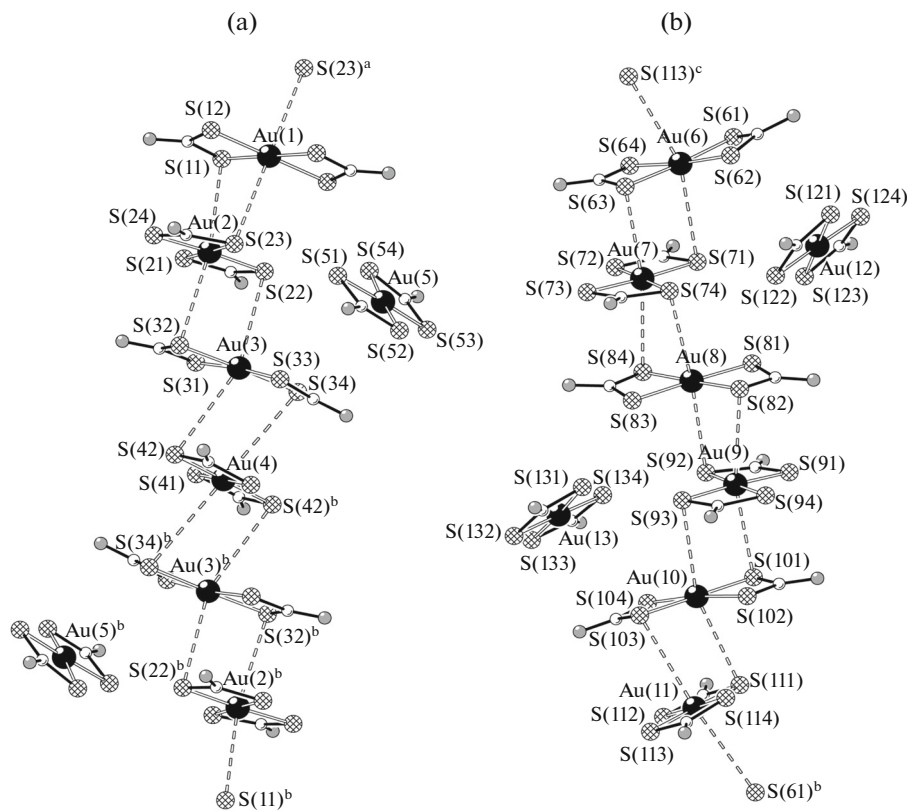


**Fig. 3.** (a, b) Full periods of two independent cation–cationic polymer chains with the accompanying discrete cations. The dashed line shows the Au···S secondary bonds. The alkyl substituents of the dithiocarbamate ligands are omitted for clarity.

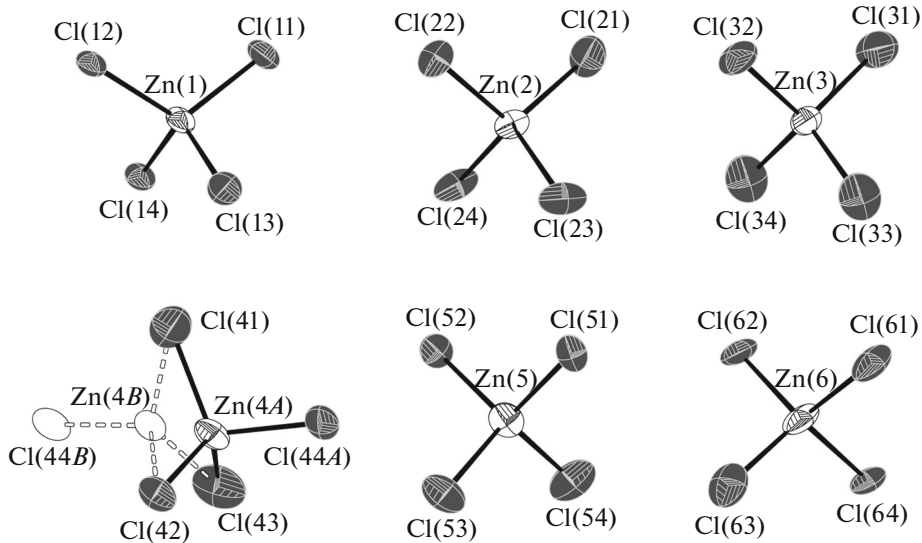


**Fig. 4.** Structure of six isomeric  $[\text{ZnCl}_4]^{2-}$  complex anions of compound I. Ellipsoids at 30% probability level.

anions allows them to be classified as conformers (Table 2).

In compound I, the isomeric  $[\text{Au}\{\text{S}_2\text{CN}(\text{C}_4\text{H}_9)_2\}_2]^+$  cations perform different struc-

tural functions. Despite the presence of electrostatic intercation repulsion forces, most of the  $[\text{Au}\{\text{S}_2\text{CN}(\text{C}_4\text{H}_9)_2\}_2]^+$  cations are involved in the formation of two sorts of long-period cation–cationic

polymer chains via pair non-valence secondary<sup>2</sup> Au···S bonds (Fig. 3). The discrete E, L, and M cations do not participate in the secondary bonds. In each complex cation, the Au···S bonds involve the central gold atom and one sulfur atom of each of the two BuDtc ligands. In most cases, these are sulfur atoms located along a diagonal in [AuS<sub>4</sub>], but in three cations (B, G, and I), the binding involves *cis*-located sulfur atom (Fig. 3). Each of the gold atoms form two Au···S bonds with neighboring cations, thus completing the [AuS<sub>4</sub>] polygon to a distorted [AuS<sub>6</sub>] octahedron. Thus, each cation forms two pairs of Au···S bonds with the close neighbors by participating in the formation of one of the two independent supramolecular chains extended along the *y* crystallographic axis, (···A···B···C···D···C···B···)<sub>*n*</sub> and (···F···G···H···I···J···K···)<sub>*n*</sub>. The Au···S distances (3.462–3.946 Å) in these chains are equal to or greater than the sum of the van der Waals radii of gold and sulfur atoms (3.46 Å [40–42]).

The formation of chains of the first type (Fig. 3a) involves four isomeric gold(III) cations: centrosymmetric A and D and non-centrosymmetric B and C cations. In the pairs of the latter cations repeated in the chain period, the [AuS<sub>4</sub>] planes are antiparallel to each other. The neighboring cations in the chain are arranged in such a way that their bisecting planes (passing through the bicyclic [CS<sub>2</sub>AuS<sub>2</sub>C] fragments) form an angle close to 90°. Discrete non-centrosymmetric cations E alternate on the left and on the right of the polymer chain (Fig. 3a). The values for the Au(1)Au(2)Au(3) (133.90°), Au(2)Au(3)Au(4) (151.11°), Au(3)Au(4)Au(3<sup>b</sup>), and Au(2)Au(1)Au(2<sup>a</sup>) (180°) angles imply the presence of linear segments in the zigzag-like chain having interatomic distances Au(1)–Au(2), 3.924 Å; Au(2)–Au(3), 4.169 Å; and Au(3)–Au(4), 4.085 Å.

The polymer chains of the second type are formed according to the same principles as the chains of the first type, but they involve six isomeric non-centrosymmetric cations F–K. The lower scatter of the values for Au(6)Au(7)Au(8) (137.24°), Au(7)Au(8)Au(9) (174.35°), Au(8)Au(9)Au(10) (138.00°), Au(9)Au(10)Au(11) (154.10°), Au(10)Au(11)Au(6) (175.41°), and Au(11)Au(6)Au(7) (151.16°) reflects a smoother character of the second zigzag-like chain, although there are no linear segments in this case; the distances in the second type chains are as follows: Au(6)–Au(7), 4.214 Å; Au(7)–Au(8), 3.928 Å; Au(8)–Au(9), 3.912 Å; Au(9)–Au(10), 4.125 Å; Au(10)–Au(11), 4.008 Å; and Au(11)–Au(6), 4.016 Å. Discrete cations K are situated strictly on one side of the chain and cations L are on the other side (Fig. 3b).

<sup>2</sup> The concept of secondary bonds was first proposed in [45] to describe the interactions at distances comparable with the sum of the van der Waals radii of the involved atoms.

The unit cell comprises altogether four full periods of first type chains and eight periods of second type chains, including the accompanying discrete cations (Fig. 2). In the neighboring chains of the second type, an opposite sequence of isomeric cations F–K is observed, i.e., the chains are antiparallel. The spatial separation of the supramolecular cation–cationic chains involves isomeric [ZnCl<sub>4</sub>]<sup>2-</sup> anions and discrete [Au{S<sub>2</sub>CN(C<sub>4</sub>H<sub>9</sub>)<sub>2</sub>}<sub>2</sub>]<sup>+</sup> cations: E, L, and M (Fig. 2).

The thermal behavior of **I** was studied by STA. The TG curve (Fig. 5a) is composed of two sections, the first one (~160–370°C) reflecting the intense weight loss as a result of thermolysis of the complex, while the other one (~370–860°C) corresponding to smooth desorption and evaporation of volatile products of thermolysis. The first steeply descending step reflects the major weight loss of 59.66% caused by the thermal destruction of the dithiocarbamate moiety with reduction of gold to the metal in the cation and liberation of ZnCl<sub>2</sub> (with partial transformation to ZnS<sup>3</sup>) in the anion. The intricate pattern of the processes is supported by the presence of inflection points in the TG curve.

The low-temperature region of the DSC curve (Fig. 5b) shows two endotherms with extreme points at 160.7 and 243.7°C. The first, more intense endotherm is attributable to melting of the compound (extrapolated mp = 159.0°C). According to an alternative determination of mp in a glass capillary, melting occurs in the temperature range of 158–160°C. The second endotherm is caused by thermolysis and almost coincides with the temperature of the maximum rate of weight loss (242.6°C) found by differentiation of the TG curve.

The second, gently sloping step of the TG curve (Fig. 5a) is associated with desorption and gradual evaporation of the products of thermolysis of **I** (8.58%) including ZnCl<sub>2</sub> (mp = 317 and bp = 733°C [47]). The residual weight at 1100°C (31.74% of the initial one) exceeds that expected for reduced gold (calcd. 27.77%) by 3.97%. This excess weight may be due to the zinc sulfide formed (sublimed at 1185°C [47]). According to full calculation of the TG curve, this corresponds to conversion of 57.8% of zinc to ZnS. The remaining 42.2% of zinc exists as ZnCl<sub>2</sub> accounting for 4.05% of the initial weight of **I**, which are included in the second stage of experimental weight loss. The high-temperature region of the DSC curve exhibits an endotherm due to gold melting with the extrapolated mp = 1063.2°C (Fig. 5b). After opening of the crucible, gold beads of 10–60 μm diameter and white zinc sulfide were found on the bottom (Fig. 5c).

<sup>3</sup> The preferred formation of metal sulfides upon the thermolysis of complexes with sulfur-containing ligands has been substantiated from the thermodynamic standpoint [46].

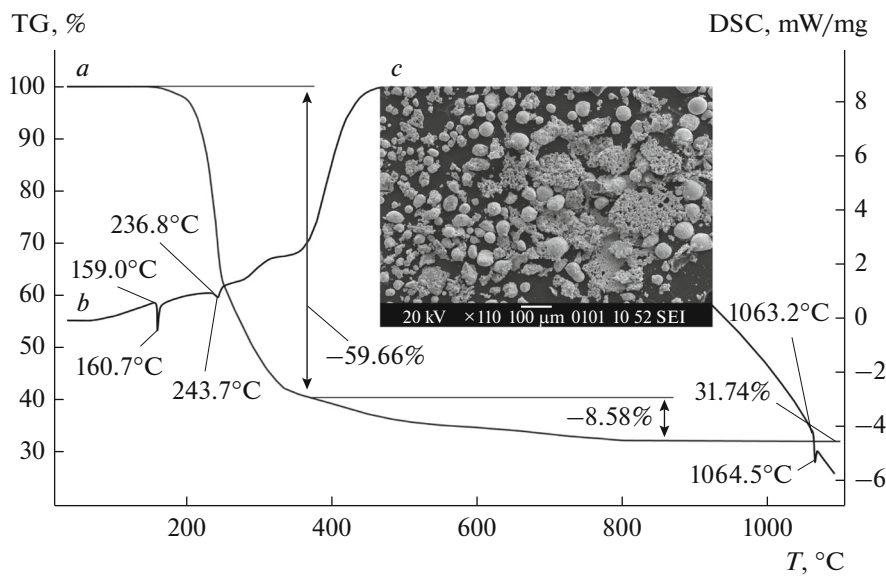


**Fig. 5.** (a) TG and (b) DSC curves for complex I. (c) Final residue of thermolysis of I consisting of ZnS and Au beads.

### ACKNOWLEDGMENTS

The authors are grateful to Professor O.N. Antzutkin (Luleå University of Technology, Luleå, Sweden) for providing the possibility to record the  $^{13}\text{C}$  MAS NMR spectra. The work was partially supported by Presidium of the Far East Branch of the RAS (Far East Program, project no. 15-I-3-001).

### REFERENCES

- Deb, M.K., Chakravarty, S., and Mishra, R.K., *J. Indian. Chem. Soc.*, 1996, vol. 73, no. 10, p. 551.
- Nieuwenhuizen, P.J., *Appl. Catal., A*, 2001, vol. 207, nos. 1-2, p. 55.
- Cicotti, M., in *Compound Class: Alkylenebis(dithiocarbamates): Handbook of Residue Analytical Methods for Agrochemicals*, Lee, P.W., Ed., Chichester: Wiley, 2003, vol. 2, p. 1089.
- Onwudiwe, D.C., Nthwane, Y.B., Ekennia, A.C., and Hosten, E., *Inorg. Chim. Acta*, 2016, vol. 447, p. 134.
- Bozdag, M., Carta, F., Vullo, D., et al., *Bioorg. Med. Chem.*, 2015, vol. 23, no. 10, p. 2368.
- Carta, F., Aggarwal, M., Maresca, A., et al., *J. Med. Chem.*, 2012, vol. 55, no. 4, p. 1721.
- Zia-ur-Rehman, Ibrahim, S., Khan, A., et al., *J. Coord. Chem.*, 2016, vol. 69, no. 3, p. 1.
- Gomathi, G., Sathiyaraj, E., Thirumaran, S., and Ciattini, S., *J. Sulfur Chem.*, 2016, vol. 37, no. 1, p. 23.
- Bharti, A., Bharati, P., Chaudhari, U.K., et al., *Polyhedron*, 2015, vol. 85, p. 712.
- Yadav, R., Trivedi, M., Kociok-Köhn, G., et al., *Eur. J. Inorg. Chem.*, 2016, no. 7, p. 1013.
- Hrubaru, M., Onwudiwe, D.C., and Hosten, E., *J. Sulfur Chem.*, 2015, vol. 37, no. 1, p. 37.
- Abdullah, N.H., Zainal, Z., Silong, S., et al., *Mater. Chem. Phys.*, 2016, vol. 173, p. 33.
- Prakasam, B.A., Lahtinen, M., Peuronen, A., et al., *Mater. Lett.*, 2015, vol. 44, p. 19.
- Loseva, O.V., Rodina, T.A., and Ivanov, A.V., *Russ. J. Coord. Chem.*, 2013, vol. 39, no. 6, p. 463.
- Ivanov, A.V., Rodina, T.A., and Loseva, O.V., *Russ. J. Coord. Chem.*, 2014, vol. 40, no. 12, p. 875.
- Ivanov, A.V., Loseva, O.V., Rodina, T.A., et al., *Russ. J. Inorg. Chem.*, 2014, vol. 59, no. 8, p. 807.
- Loseva, O.V. and Ivanov, A.V., *Russ. J. Inorg. Chem.*, 2014, vol. 59, no. 12, p. 1491.
- Loseva, O.V., Rodina, T.A., Smolentsev, A.I., and Ivanov, A.V., *J. Struct. Chem.*, 2014, vol. 55, no. 5, p. 901.
- Rodina, T.A., Loseva, O.V., Smolentsev, A.I., and Ivanov, A.V., *J. Struct. Chem.*, 2016, vol. 42, no. 1, p. 146.
- Byr'ko, V.M., *Ditiokarbamaty* (Dithiocarbamates), Moscow: Nauka, 1984.
- Ivanov, A.V., Ivakhnenko, E.V., Gerasimenko, A.V., and Forsling, W., *Russ. J. Inorg. Chem.*, 2003, vol. 48, no. 1, p. 45.
- Zhong, Y., Zhang, W.G., Zhang, Q.J., et al., *Acta Chim. Sin.*, 2003, vol. 61, no. 11, p. 1828.
- Klug, H.P., *Acta Crystallogr.*, 1966, vol. 21, no. 4, p. 536.
- Bonamico, M., Mazzone, G., Vaciago, A., and Zambonelli, L., *Acta Crystallogr.*, 1965, vol. 19, no. 6, p. 898.
- Sreehari, N., Varghese, B., and Manoharan, P.T., *Inorg. Chem.*, 1990, vol. 29, no. 20, p. 4011.
- Miyamae, H., Ito, M., and Iwasaki, H., *Acta Crystallogr., Sect. B: Struct. Crystallogr., Cryst. Chem.*, 1979, vol. 35, p. 1480.
- Kellö, E., Vrabel, V., Kettmann, V., and Garaj, J., *Collect. Czech. Chem. Commun.*, 1983, vol. 48, p. 1272.
- Francetić, V. and Leban, I., *Vestn. Slov. Kem. Drus.*, 1979, vol. 26, p. 113.

29. Agre, V.M. and Shugam, E.A., *Zh. Strukt. Khim.*, 1972, vol. 13, no. 4, p. 660.
30. Motevalli, M., O'Brien, P., Walsh, J.R., and Watson, I.M., *Polyhedron*, 1996, vol. 15, no. 16, p. 2801.
31. Cox, M.J. and Tiekkink, E.R.T., *Z. Kristallogr.*, 1999, vol. 214, no. 3, p. 184.
32. Tiekkink, E.R.T., *CrystEngComm*, 2003, vol. 5, no. 21, p. 101.
33. Ivanov, A.V., Korneeva, E.V., Gerasimenko, A.V., and Forsling, W., *Russ. J. Coord. Chem.*, 2005, vol. 31, no. 10, p. 695.
34. Ivanov, A.V. and Antzutkin, O.N., *Topics Curr. Chem.*, 2005, vol. 246, p. 271.
35. Shaheen, F., Gieck, C., Badshah, A., and Khosa, M.K., *Acta Crystallogr., Sect. E: Struct. Rep. Online*, 2006, vol. 62, no. 6, p. m1186.
36. Shahid, M., Ruffer, T., Lang, H., et al., *J. Coord. Chem.*, 2009, vol. 62, no. 3, p. 440.
37. Ferreira, I.P., de Lima, G.M., Paniago, E.B., et al., *Inorg. Chim. Acta*, 2016, vol. 441, p. 137.
38. Pines, A., Gibby, M.G., and Waugh, J.S., *J. Chem. Phys.*, 1972, vol. 56, no. 4, p. 1776.
39. *APEX2 (version 1.08), SAINT (version 7.03), SADABS (version 2.11) and SHELXTL (version 6.12)*, Madison: Bruker AXS Inc., 2004.
40. Pauling, L., *The Nature of the Chemical Bond and the Structure of Molecules and Crystals*, London: Cornell Univ., 1960.
41. Bondi, A., *J. Phys. Chem.*, 1964, vol. 68, no. 3, p. 441.
42. Bondi, A., *J. Phys. Chem.*, 1966, vol. 70, no. 9, p. 3006.
43. Exarchos, G., Robinson, S.D., and Steed, J.W., *Polyhedron*, 2001, vol. 20, nos. 24–25, p. 2951.
44. Karâa, N., Hamdi, B., Ben Salah, A., and Zouari, R., *J. Mol. Struct.*, 2013, vol. 1049, nos. 1–3, p. 48.
45. Alcock, N.W., *Adv. Inorg. Chem. Radiochem.*, 1972, vol. 15, no. 1, p. 1.
46. Razuvayev, G.A., Almazov, G.V., Domrachev, G.A., et al., *Dokl. Akad. Nauk SSSR*, 1987, vol. 294, no. 1, p. 141.
47. Lidin, R.A., Andreeva, L.L., and Molochko, V.A., *Spravochnik po neorganicheskoi khimii* (Handbook in Inorganic Chemistry), Moscow: Khimiya, 1987.

*Translated by Z. Svitanko*